HHS Public Access

Author manuscript

Microbes Infect. Author manuscript; available in PMC 2015 November 01.

Published in final edited form as:

Microbes Infect. 2014 November ; 16(11): 893–901. doi:10.1016/j.micinf.2014.08.006.

Adipocytes in both brown and white adipose tissue of adult mice are functionally connected via gap junctions: implications for Chagas disease

Shoshana Burke[a,b], **Fnu Nagajyothi**[b], **Mia M. Thi**[a,c], **Menachem Hanani**[e], **Philipp E. Scherer**[f], **Herbert B. Tanowitz**[b,d], and **David C. Spray**[a,d,*]

[a]Department of Neuroscience, Albert Einstein College of Medicine, Bronx, NY 10461, USA

[b]Department of Pathology, Albert Einstein College of Medicine, Bronx, NY 10461, USA

[c]Department of Orthopedic Surgery, Albert Einstein College of Medicine, Bronx, NY 10461, USA

[d]Department of Medicine, Albert Einstein College of Medicine, Bronx, NY 10461, USA

[e]Laboratory of Experimental Surgery, Hadassah-Hebrew University- Medical Center, Mount Scopus, Jerusalem, 91120, Israel

[f]Department of Internal Medicine and Cell Biology and the Touchstone Diabetes Center, University of Texas Southwestern Medical Center, Dallas, TX

Abstract

Adipose tissue serves as a host reservoir for the protozoan *Trypanosoma cruzi*, the causative organism in Chagas disease. Gap junctions interconnect cells of most tissues, serving to synchronize cell activities including secretion in glandular tissue, and we have previously demonstrated that gap junctions are altered in various tissues and cells infected with *T. cruzi*. Herein, we examined the gap junction protein connexin 43 (Cx43) expression in infected adipose tissues. Adipose tissue is the largest endocrine organ of the body and is also involved in other physiological functions. In mammals, it is primarily composed of white adipocytes. Although gap junctions are a prominent feature of brown adipocytes, they have not been explored extensively in white adipocytes, especially in the setting of infection. Thus, we examined functional coupling in both white and brown adipocytes in mice. Injection of electrical current or the dye Lucifer Yellow into adipocytes within fat tissue spread to adjacent cells, which was reduced by treatment with agents known to block gap junctions. Moreover, Cx43 was detected in both brown and white fat tissue. At thirty and ninety days post-infection, Cx43 was downregulated in brown adipocytes and upregulated in white adipocytes. Gap junction-mediated intercellular communication likely contributes to hormone secretion and other functions in white adipose tissue and to nonshivering

*Correspondent footnote: David C. Spray, Ph.D., Albert Einstein College of Medicine, 1300 Morris Park Avenue, Kennedy, Room 840, Bronx, New York 10461, Tel: (718) 430-2537, Fax: (718) 430-8594, david.spray@einstein.yu.edu.

thermogenesis in brown fat, and modulation of the coupling by *T. cruzi* infection is expected to impact these functions.

Keywords

Trypanosoma cruzi; Chagas disease; gap junctions; adipose tissue; white adipose tissue; brown adipose tissue; connexin43

Abbreviations

Cx43; WAT; BAT; *T. cruzi*

1. Introduction

Gap junctions provide intercellular channels that mediate diffusional exchange of ions, signaling molecules and metabolites (up to 1kDa) between cells of most tissues. Gap junction channels are formed by paired connexons or hemichannels, each made up of six connexin (Cx) subunits. Gap junctions in excitable tissues such as heart and brain provide rapid and synchronized cellular activity, and in most other cell types share intercellular metabolites and contribute large effective cell volume to buffer toxins, being both protectors and executioners in Bystander cell killing [1]. Importantly, gap junctions connect cells of most glandular tissues, where the gap junction proteins (connexins) and/or the intercellular spread of small molecules through gap junction channels play critical roles in optimizing secretion in both endocrine and exocrine glands [2].

Adipose tissue, the largest endocrine organ in the body, is primarily regarded as the storage site for lipids. However, it also contributes to energy homeostasis and immune responses including those activated by infection [3, 4]. Adipocytes exert their influence through the synthesis and release of tissue-specific adipokines as well as cytokines and chemokines. Most of the fat deposits in the body consist of white adipose tissue (WAT). Brown adipose tissue (BAT) was originally thought to function primarily in neonatal animals, where its mitochondria and lipid droplet-rich cells provide critical nonshivering thermogenesis. However, positron emission tomography (PET) scan studies revealed significant BAT in normal adult humans indicating that BAT plays a metabolic role also in adults [5].

There have been very few studies of gap junctions in adipose tissue, despite their potential importance in systemic physiology and pathology. Gap junctions are recognized as interconnecting adipose cells in BAT, as evidenced using electron microscopic and electrophysiological techniques [6–8]. There is far less conclusive evidence on gap junctions in WAT, although weak coupling in amphibian white adipocytes has been reported [8]. Thus, we examined whether such coupling is also present in mammalian WAT, which may have important implications to secretion [2] and possibly other functions of this tissue. Herein, we demonstrate the presence of gap junctions in mouse WAT which contrasts with interpretation from cell culture studies of NIH 3T3 preadipoytes, where it has been speculated that expression of the gap junction protein connexin 43 (Cx43) interferes with adipocyte differentiation and adipogenesis [9, 10].

Gap junction expression and function are altered in numerous disease states, both hereditary and acquired [11]. We have found that infection with *Trypanosoma cruzi*, the causative agent of Chagas disease, alters gap junction expression in cultured cells obtained from heart and brain [12–14]. In *T. cruzi*-infected adipose tissue and cultured adipocytes there is upregulation of inflammatory mediators [15–18]. These findings prompted our investigation of the question of whether there is a role for adipose tissue gap junctions in response to *T. cruz*i infection. This is important because the intercellular communication that gap junction channels provide can serve to spread injury from damaged cells to “Bystanders” or to rescue dying cells from toxicity [1]. Furthermore, gap junction expression and function are modified by inflammatory mediators, and our laboratory has demonstrated alterations in gap junctions in various tissues and cells infected with *T. cruzi* [12]. To explore the impact of *T. cruzi* infection on intercellular communication in adipose tissue, we studied adipose tissue of infected and uninfected mice and compared changes in gap junctions in BAT and WAT. Our findings that gap junctions in WAT and BAT are oppositely regulated by *T. cruzi* infection could have important implications in adipose tissue pathophysiology in the setting of Chagas disease.

2. Materials and Methods

2.1. Parasitology

The Brazil strain of *T. cruzi* was maintained in C3H mice (Jackson Laboratories, Bar Harbor, ME, USA). Male CD-1 mice (Charles River, Wilmington, MA, USA) 8 to 10 weeks old (weighing 25–35 g) were infected intraperitoneally with 5×10^4 trypomastigotes. In this model, the parasitemia increases 20 to 35 days post infection (dpi) (acute stage) and gradually wanes by day 40 to 45 dpi. There is a 50% mortality rate during the acute stage of infection. Surviving mice enter the chronic stage, and by 90 to 100 dpi there is a profound cardiomyopathy as determined by histopathology and cardiac imaging studies [18, 19]. Additionally, we have detected the presence of parasites in the adipose tissue in both acutely and chronically infected mice [15]. Thirty and 90 dpi, sex and aged-matched control and infected CD-1 mice were sacrificed, and interscapular BAT and epididymal and mesenteric WAT were utilized in this study.

2.2. Tissue Preparation

Mice were housed in AALAC approved animal facilities and were killed by asphyxiation and cervical dislocation, as approved by our Institution’s animal use committee. BAT was dissected from interscapular fat pad and WAT from both epididymus and mesentery. Epididymal WAT was used for Western blots and immunostaining, whereas mesenteric WAT was used for dye injection and electrophysiology due to its composition almost entirely of adipocytes and its thinness, being only a few cell layers thick. BAT and mesenteric WAT segments were slightly stretched and pinned to a Sylgard (Dow Corning, Midland, MI, USA) coated dish using cactus spines or fine insect pins and continuously superfused with Krebs solution containing (in mM) NaCl (110), KCl (4.7), $NaHCO_3$ (14.4), $MgSO_4$ (1.2), NaH_2PO_4 (1.2), $CaCl_2$ (2.5) and glucose (11.5), at pH 7.3 and bubbled with 95%O_2/ 5% CO_2.

2.3. Dye coupling and electrophysiology

Experiments were performed using an upright microscope (Nikon Eclipse EC600FN) equipped with fluorescent illumination and a digital camera (Micrometrix 590 CU, 5M; Beijing, China) connected to a computer running proprietary imaging software. Mouse BAT and WAT were collected as described above. Individual adipocytes visualized in the pinned tissue were injected with the fluorescent dye Lucifer yellow (LY, Sigma, St. Louis, MO, USA) 2.5% in 0.5 M LiCl from micropipettes connected to a preamplifier (Molecular Devices). Tip resistances of microelectrodes were 80–120 MΩ. LY was injected intracellularly by negative 5nA, 100 msec current pulses at 5 Hz for 5 min [20, 21]. During and after LY injections, the dye-injected cells and their neighbors were imaged with the digital camera. To assure that coupling was mediated by gap junctions, samples were pre-incubated with the gap junction channel blocker 1-heptanol (3mM) for 1 h. A total of 5–17 tissue samples were used for each type of experiment (one tissue sample per animal) and 3–15 cells were injected in each tissue sample to quantify the extent of dye coupling under control and heptanol blockade conditions.

To measure electrical coupling, two adjacent adipocytes were impaled with sharp microelectrodes that were filled with 3 M KCl and connected to Axoclamp electrometers with bridge balance control. Current pulses were injected into one cell of the pair while recording voltages in both cells. To control for high resistance to ground that might result from tight extracellular space and could be misinterpreted as actual electrical coupling, recordings were obtained under conditions where only one electrode or neither was intracellular. In no case was apparent coupling detected under these conditions (see Fig. 2C).

2.3. Immunostaining and confocal microscopy

Freshly isolated BAT and WAT whole mounts were fixed in 4% paraformaldehyde overnight at 4°C and washed with phosphate buffered saline (PBS, pH 7.4) for 2 h. To block free aldehyde groups, the tissues were incubated with 50 mM ammonium chloride for 30 min at room temperature (RT). Tissues were then permeabilized using Proteinase K (20 μg/ml in 10mM tris-HCl) for 5 min at RT and 100% methanol for 5 min at −20°C. Non-specific bind ing was blocked using 1% bovine serum albumin (BSA) in PBS with 0.3% Triton-X. Tissues were then incubated with primary antibodies for 48 h at 4°C followed by 2 h secondary antibody incubation at RT with intervening washes. The rabbit polyclonal primary antibody against Cx43 (Sigma-Aldrich, St Louis, MO, USA),1:500 and secondary antibody anti-rabbit tagged with Alexa 488 (Invitrogen, Grand Island, NY, USA), 1:400 were used. As a control for non-specific staining, primary antibody was omitted in same experiments (see Suppl. Fig. 1). Lipids were stained with Oil-Red-O (Sigma-Aldrich) in 60% propanol for 20 min and nuclear DNA was stained with 4', 6-diamidino-2-phenylindole (DAPI, Sigma-Aldrich). Images were acquired with Zeiss LSM 510 Duo laser scanning confocal microscope (Carl Zeiss NY, USA) using a 40× water-immersion objective. Images were acquired serially from top to bottom of each image field using a ‘z’ plane motorized sub-stage. The upper and lower z-axis positions were selected so that the entire thickness of either BAT or WAT was imaged in each series. Image stacks of tissue samples were collected at 0.9 μm z-axis steps.

2.4. Western Blot

BAT and WAT were collected, frozen in liquid nitrogen and stored at −80°C until further use. For Western blot analysis, protein lysates (30–40 μg) were prepared from frozen tissues in buffer containing 1 mM sodium bicarbonate, 1 mM sodium orthovanadate, 5 mM EDTA, with a mixture of protease inhibitor [2mM phenylmethylsulfonyl fluoride (PMSF) and Complete Protease Inhibitor Cocktail (Roche Applied Science, Indianapolis, IN, USA)], sonicated and resolved by sodium dodecyl sulfate polyacrylamide gel electrophoresis on 10% acrylamide gels, and transferred to nitrocellulose membrane (Whatman, Dassel, Germany). Blots were probed with primary antibodies to rabbit anti Cx43 (C6219: Sigma-Aldrich), 1:20,000 for 3 days at 4°C, followed by secondary antibody incubation with horseradish peroxidase (HRP)-conjugated anti-rabbit IgG (Santa Cruz Biotechnology, CA, USA), 1:10,000 for 1 h at RT. Blots were reprobed with mouse anti glyceraldehyde 3-phosphate dehydrogenase (GAPDH, Fitzgerald, Acton, MA, USA), 1:10,000 for 1 h at RT followed by secondary HRP-conjugated mouse IgG. Protein bands were detected using Immobilon Western Chemiluminescent HRP Substrate kit (EMD Millipore Corporation, Billerica, MA, USA). Immunoblots from a minimum of 3 independent experiments were scanned using In-Vivo F PRO imaging system (Bruker, CT, USA), and the background-corrected signal from each band was quantified by densitometry using Image J software (NIH, USA). Signal sfor each sample lane were first normalized to the internal loading control GAPDH, then normalized to the respective control.

2.5. Statistical analysis

The normalized relative levels for each experimental group were compared to controls and are presented as the means ±SEM. GraphPad Prism 6 (GraphPad Software, Inc., La Jolla, CA, USA) was used to perform either *t*-tests or one way ANOVA followed by Tukey's multiple comparison tests to compare test and control groups. $P<0.05$ was considered to be statistically significant.

3. Results

3.1. Functional coupling among brown and among white adipocytes

Coupling among adipocytes was assessed by intracellular Lucifer yellow injection. BAT cells were found to be coupled to an average of 3.3 ± 0.3 (N = 9) other cells 5 min after injection (Fig. 1A,B,C and Fig. 2A,B). Injection of Lucifer yellow into WAT cells revealed single lipid droplet in spherically shaped cells surrounded by LY dye. The extent of coupling in WAT cells was less than in BAT, and on average only about one (0.9 ± 0.1; N = 17) other cell was labeled (Fig. 1D,E,F and Fig. 2A,B). To test whether the dye transfer was mediated by gap junctions, we exposed the tissue to 3 mM heptanol for 1 h and then performed dye coupling experiments. For both BAT (N=5) and WAT (N=5), heptanol treatment significantly reduced dye spread (Fig. 2 A,B).

An alternative method for measuring functional coupling was performed with microelectrodes inserted into two adjacent cells. As illustrated in Fig. 2C, for both brown and white fat cells, junctional spread of current was recorded under these conditions, which was not present when one electrode was within a cell and the other in the tissue but not

inside a cell (top panel). This electrical coupling was blocked after treatment of tissue with 3 mM heptanol (bottom panel). Coupling coefficients (calculated as the voltage in cell 2 divided by the voltage in cell 1) were significantly higher for BAT than WAT (0.4±0.1 vs 0.17±0.03) and were reduced by ten fold or more heptanol treatment (to 0.04±0.03 in BAT and to 0.01±0.01 in WAT). These findings of heptanol blockable dye and electrical coupling indicate that gap junction mediated intercellular communication is present between adipose cells of both BAT and WAT.

3.2. Cx43 is present in WAT and BAT

Cx43 has been previously reported to be the major gap junction protein in BAT, where it is upregulated during hibernation in ground squirrels [22]; it is also the major gap junction protein expressed in NIH3T3 cells, commonly used as a preadipocyte cell line in which adipogenesis can be experimentally induced (see [9]). To determine the distribution of Cx43 in BAT and WAT, we stained both tissues with Cx43 antibodies and counterstained with Oil-Red-O (ORO) to label lipid droplets, and with DAPI to label nuclei. Note absence of punctate staining of appositional membrane of either BAT or WAT when primary antibody was omitted (Suppl. Fig. 1). As shown in Fig. 3A, when stained with Cx43 specific antibody, BAT expressed Cx43 abundantly at many cellular interfaces in cells stained with ORO. When WAT was stained with the same antibodies, we found much lower Cx43 expression at the interfaces of ORO labeled cells, indicating that WAT adipocytes expressed Cx43, although less than BAT (Fig. 3B). To verify the presence of Cx43 in BAT and WAT and compare expression levels, we performed Western blots on tissue samples using the same antibody as used for immunostaining. As shown in Fig. 3C, Cx43 level in WAT was significantly lower than in BAT.

3.3. Effects of T. cruzi infection on Cx43 expression in BAT and WAT

To determine the effect of acute *T. cruzi* infection on Cx43 expression, we stained BAT and WAT with Cx43 antibodies at 30 dpi. Comparison between infected tissues and those from age-matched control mice is shown in Fig. 4. We noted that the normally strong Cx43 staining in BAT was much reduced in the infected mice (Fig. 4A). In contrast, Cx43 expression in the infected WAT was significantly higher compared with uninfected control tissue (Fig. 4B). To quantitatively compare the effect of infection on Cx43 expression in BAT and WAT, we performed Western blots on the tissues, as shown in Fig. 4A,B (right panel). Quantification of signals first normalized for GAPDH levels followed by respective controls revealed that at 30 dpi resulted Cx43 levels were reduced in BAT by 80% while there was a 50% increase in Cx43 levels in WAT In both cases, the changes were statistically significant.

3.4. Effects of 90 day T. cruzi infection on Cx43 expression in BAT and WAT

To determine the effect of chronic *T. cruzi* infection on Cx43 expression, we stained BAT and WAT with Cx43 antibodies 90 dpi. As with 30 dpi mice, the chronic infection resulted in reduced expression of Cx43 in BAT (Fig. 5A) and increased expression in WAT (Fig. 5B). Quantitation of expression levels using Western blots revealed significantly lower

expression (~ 50% less) in 90 day infected BAT and about 25% increase in Cx43 expression in infected WAT. In both cases, the changes were statistically significant.

4. Discussion

Gap junctions are virtually ubiquitous in body tissues. However, their expression and functional importance in WAT has not been extensively studied. Herein, we report the presence of the gap junction protein Cx43 and functional coupling in mammalian WAT and we propose that like in other tissues, gap junctions play important roles in the physiology and pathophysiology of both types of adipose tissue.

Using the 3T3-L1 preadipocyte cell line [23], it has been reported that Cx43 hyperphosphorylation and degradation are required for differentiation [9]. This is consistent with reports that MC3T3-E1 preosteoblast transdifferentiation to adipocytes was favored when gap junction coupling was blocked [24] and that H-1/A marrow stromal cells lost dye coupling as they differentiated into adipocytes [25]. However, several previous studies have demonstrated electrical and dye coupling as well as gap junctions between adipocytes in BAT [7, 8, 26] and our dye injections, electrical recordings and Cx43 immunostaining clearly show the presence and functional coupling of gap junction in WAT. These findings therefore provide further support to the growing understanding that adipose tissue is a very sophisticated organ, far more than just an inert storage/expenditure compartment for lipids.

Studies untilizing cultured adipocytes have been carried out on cultured cells [27, 28], more frequently compared to studies with intact adipose tissue. However, BAT and WAT from mice offer considerable advantages because in these preparations the *in vivo* organization of the cells is preserved, including cell connectivity and the local innervation. We thus were able to demonstrate both dye and electrical coupling in freshly isolated tissues. These interactions are likely to be substantially altered under tissue culture conditions, which is difficult from primary cells because fat tissue floats. These observations were fully supported by immunohistochemistry and Western blot studies. Further work on isolated fat tissues both normal mice and mouse disease models (e.g., Chagas disease model) and from infected mice in which adipocyte Cx43 is deleted will likely contribute to the understanding of roles of gap junctions in adipocytes.

Moreover, our results indicate that *T. cruzi* infection of adipose tissue has opposite effects on the gap junctions interconnecting the adipocytes, increasing Cx43 expression in WAT and decreasing it in BAT. It is known that several pathogens may reside in fat cells, exploiting an energy rich tissue niche [29–31], and one such example is *T. cruzi*, the causative agent of Chagas disease. As gap junctions are a target in Chagas disease [12], and loss of gap junctions impacts the various functions of adipose tissue including endocrine, immune and energy homeostasis. Reversing these changes may be expected to ameliorate certain aspects of the disease process.

Major issues remaining are the cause of the alterations in Cx43 expression and consequences for the endocrine, energy storing and thermogenic functions that fat performs. While the function of gap junctions in excitable cells is to synchronize activity of neurons, and

nonskeletal muscles (e.g., heart and smooth muscle), function in other tissues is less clear. However, one of the most solidly established functions for gap junctions is in synchronizing endocrine cells, thereby optimizing secretion [2], and the endocrine functions that fat performs are likely optimized by the intercellular gap junction mediated coupling. Modulation of this coupling under various physiological and pathological conditions may influence the function of adipose tissue. It was found that coupling by gap junctions is altered by inflammation [32] and by chemotherapeutic drugs [33]. If this also holds for coupling in adipose tissue, it might have far-reaching clinical implications.

After infection with *T. cruzi*, intracellular amastigote forms are observed both in the acute and chronic phases and in both WAT and BAT. The studies of Shoemaker and colleagues in the 1970s suggested preference for BAT in *T. cruzi* (Tulahuen strain) infected mice [34, 35]. However, we have found that as early as 15 days after infection of mice with *T. cruzi* (Brazil strain), there is a significant parasite load in both BAT and WAT as compared with other organs such the heart and spleen [36]. Macrophages and parasites are found in adipose tissue in mice chronically infected with *T. cruzi*, and the parasite persisted for over 300 days [15]. Recently, it was verified that *T. cruzi* persists in adipose tissue of chronic Chagasic patients [16].

We have shown previously that gap junctions are a target in Chagas disease [12]. It has been thought that this is at least partially responsible for the cardiac conduction deficits seen in Chagasic heart disease. Studies in cultured mouse cardiac myocytes infected with *T. cruz*i demonstrated that Cx43 immunofluorescence between infected cells was substantially lower after infection, whereas coupling between non-parasitized cells in infected dishes was not affected [37]. However, the results reported here indicate that previous conclusions may be tissue specific, since the changes we observed in BAT and WAT are opposite.

As to the mechanism responsible for changes in Cx43 expression, a major consequence of *T. cruzi* infection is the induction of inflammation, and numerous studies have now reported that IL-1β may up- or downregulate Cx43, depending on tissue [38–41]. Previously, we have demonstrated both by Western blotting and PCR analyses that *T. cruzi* infection of mice results in the increased expression of proinflammatory cytokines and chemokines including IL-1β [15, 36]. At both 30 and 90 days of infection there is a greater increase in proinflammatory cytokines and chemokines in BAT than in WAT (Nagajyothi et al, unpublished observations), and thus the observed reduction in Cx43 expression in BAT obtained from *T. cruzi*-infected mice may be explained in part by the increased expression of pro-inflammatory mediators such as IL-1β.

The mechanism responsible for increased expression of Cx43 in infected WAT remains to be fully explained. White and brown adipocytes differ morphologically and with regard to principal physiological functions, and differential response of Cx43 expression in these tissues could simply reflect tissue specific differences in signaling pathways. Although parasites exhibit higher affinity for both brown and white adipocytes than to other tissues at the early acute phase of *T. cruzi* infection in mice, white adipocytes are the major targets. We have observed that infection leads to a significant and continuous loss in WAT due to lipolysis that is greater than in BAT [36]. Given that Cx43 expression and function are

crucial to adipogenesis [23] and the plasticity of white adipocytes [42, 43], increased Cx43 in infected white adipocytes could reflect pathological remodeling in that tissue.

Supplementary Material

Refer to Web version on PubMed Central for supplementary material.

Acknowledgments

We wish to thank Dahzi Zhao for technical assistance. This work was supported by National Institutes of Health T32 AI070117 to SB, AI076248 to HBT, DK091466 to MMT, AR057139 to DCS and MMT, HL112099 to FN and NBT and by the US-Israel Binational Science Foundation 2011044 to DCS and MH.

References

1. Spray DC, Hanstein R, Lopez-Quintero SV, Stout RF Jr, Suadicani SO, Thi MM. Gap junctions and Bystander Effects: Good Samaritans and executioners. Wiley Interdiscip Rev Membr Transp Signal. 2013; 2:1–15. [PubMed: 23565352]
2. Michon L, Nlend Nlend R, Bavamian S, Bischoff L, Boucard N, Caille D, Cancela J, Charollais A, Charpantier E, Klee P, Peyrou M, Populaire C, Zulianello L, Meda P. Involvement of gap junctional communication in secretion. Biochim Biophys Acta. 2005; 1719:82–101. [PubMed: 16359942]
3. Halberg N, Wernstedt-Asterholm I, Scherer PE. The adipocyte as an endocrine cell. Endocrinol Metab Clin North Am. 2008; 37:753–768. x–xi. [PubMed: 18775362]
4. Scherer PE. Adipose tissue: from lipid storage compartment to endocrine organ. Diabetes. 2006; 55:1537–1545. [PubMed: 16731815]
5. Nedergaard J, Bengtsson T, Cannon B. Unexpected evidence for active brown adipose tissue in adult humans. Am J Physiol Endocrinol Metab. 2007; 293:E444–E452. [PubMed: 17473055]
6. Linck G, Stoeckel ME, Porte A, Petrovic A. Demonstration of gap junctions or nexus by lanthanum in the brown fat of the European hamster (Cricetus cricetus). C R Acad Sci Hebd Seances Acad Sci D. 1974; 278:87–89. [PubMed: 4211377]
7. Revel JP, Sheridan JD. Electrophysiological and ultrastructural studies of intercellular junctions in brown fat. J Physiol. 1968; 194:34P–35P.
8. Sheridan JD. Electrical coupling between fat cells in newt fat body and mouse brown fat. J Cell Biol. 1971; 50:795–803. [PubMed: 4938627]
9. Yeganeh A, Stelmack GL, Fandrich RR, Halayko AJ, Kardami E, Zahradka P. Connexin 43 phosphorylation and degradation are required for adipogenesis. Biochim Biophys Acta. 2012; 1823:1731–1744. [PubMed: 22705883]
10. Chao LC, Bensinger SJ, Villanueva CJ, Wroblewski K, Tontonoz P. Inhibition of adipocyte differentiation by Nur77, Nurr1, and Nor1. Mol Endocrinol. 2008; 22:2596–2608. [PubMed: 18945812]
11. Lai-Cheong JE, Arita K, McGrath JA. Genetic diseases of junctions. J Invest Dermatol. 2007; 127:2713–2725. [PubMed: 18007692]
12. Adesse D, Goldenberg RC, Fortes FS, Jasmin Iacobas DA, Iacobas S, Campos de Carvalho AC, de Narareth Meirelles M, Huang H, Soares MB, Tanowitz HB, Garzoni LR, Spray DC. Gap junctions and chagas disease. Adv Parasitol. 2011; 76:63–81. [PubMed: 21884887]
13. Campos de Carvalho AC, Roy C, Hertzberg EL, Tanowitz HB, Kessler JA, Weiss LM, Wittner M, Dermietzel R, Gao Y, Spray DC. Gap junction disappearance in astrocytes and leptomeningeal cells as a consequence of protozoan infection. Brain Res. 1998; 790:304–314. [PubMed: 9593958]
14. de Carvalho AC, Tanowitz HB, Wittner M, Dermietzel R, Roy C, Hertzberg EL, Spray DC. Gap junction distribution is altered between cardiac myocytes infected with *Trypanosoma cruzi*. Circ Res. 1992; 70:733–742. [PubMed: 1551199]
15. Combs TP, Nagajyothi Mukherjee S, de Almeida CJ, Jelicks LA, Schubert W, Lin Y, Jayabalan DS, Zhao D, Braunstein VL, Landskroner-Eiger S, Cordero A, Factor SM, Weiss LM, Lisanti MP,

Tanowitz HB, Scherer PE. The adipocyte as an important target cell for *Trypanosoma cruzi* infection. J Biol Chem. 2005; 280:24085–24094. [PubMed: 15843370]

16. Ferreira AV, Segatto M, Menezes Z, Macedo AM, Gelape C, de Oliveira Andrade L, Nagajyothi F, Scherer PE, Teixeira MM, Tanowitz HB. Evidence for *Trypanosoma cruzi* in adipose tissue in human chronic Chagas disease. Microbes Infect. 2011; 13:1002–1005. [PubMed: 21726660]
17. Nagajyothi F, Machado FS, Burleigh BA, Jelicks LA, Scherer PE, Mukherjee S, Lisanti MP, Weiss LM, Garg NJ, Tanowitz HB. Mechanisms of *Trypanosoma cruzi* persistence in Chagas disease. Cell Microbiol. 2012; 14:634–643. [PubMed: 22309180]
18. Tanowitz HB, Jelicks LA, Machado FS, Esper L, Qi X, Desruisseaux MS, Chua SC, Scherer PE, Nagajyothi F. Adipose tissue, diabetes and Chagas disease. Adv Parasitol. 2011; 76:235–250. [PubMed: 21884894]
19. Jelicks LA, Lisanti MP, Machado FS, Weiss LM, Tanowitz HB, Desruisseaux MS. Imaging of small-animal models of infectious diseases. Am J Pathol. 2013; 182:296–304. [PubMed: 23201133]
20. Hanani M. Lucifer yellow - an angel rather than the devil. J Cell Mol Med. 2012; 16:22–31. [PubMed: 21740513]
21. Thi MM, Urban-Maldonado M, Spray DC, Suadicani SO. Characterization of hTERT-immortalized osteoblast cell lines generated from wild-type and connexin43-null mouse calvaria. Am J Physiol Cell Physiol. 2010; 299:C994–C1006. [PubMed: 20686067]
22. Yan J, Burman A, Nichols C, Alila L, Showe LC, Showe MK, Boyer BB, Barnes BM, Marr TG. Detection of differential gene expression in brown adipose tissue of hibernating arctic ground squirrels with mouse microarrays. Physiol Genomics. 2006; 25:346–353. [PubMed: 16464973]
23. Yanagiya T, Tanabe A, Hotta K. Gap-junctional communication is required for mitotic clonal expansion during adipogenesis. Obesity (Silver Spring). 2007; 15:572–582. [PubMed: 17372306]
24. Schiller PC, D'Ippolito G, Brambilla R, Roos BA, Howard GA. Inhibition of gap-junctional communication induces the trans-differentiation of osteoblasts to an adipocytic phenotype in vitro. J Biol Chem. 2001; 276:14133–14138. [PubMed: 11278824]
25. Umezawa A, Hata J. Expression of gap-junctional protein (connexin 43 or alpha-1 gap junction) is down-regulated at the transcriptional level during adipocyte differentiation of H-1/A marrow stromal cells. Cell Struct Funct. 1992; 17:177–184. [PubMed: 1322801]
26. Revel JP, Yee AG, Hudspeth AJ. Gap junctions between electrotonically coupled cells in tissue culture and in brown fat. Proc Natl Acad Sci U S A. 1971; 68:2924–2927. [PubMed: 5289236]
27. Lafontan M. Historical perspectives in fat cell biology: the fat cell as a model for the investigation of hormonal and metabolic pathways. Am J Physiol Cell Physiol. 2012; 302:C327–C359. [PubMed: 21900692]
28. Trayhurn P. Hypoxia and adipose tissue function and dysfunction in obesity. Physiol Rev. 2013; 93:1–21. [PubMed: 23303904]
29. Hazan U, Romero IA, Cancello R, Valente S, Perrin V, Mariot V, Dumonceaux J, Gerhardt CC, Strosberg AD, Couraud PO, Pietri-Rouxel F. Human adipose cells express *CD4*, *CXCR4*, and *CCR5* [corrected] receptors: a new target cell type for the immunodeficiency virus-1? FASEB J. 2002; 16:1254–1256. [PubMed: 12153994]
30. Bechah Y, Paddock CD, Capo C, Mege JL, Raoult D. Adipose tissue serves as a reservoir for recrudescent Rickettsia prowazekii infection in a mouse model. PLoS One. 2010; 5:e8547. [PubMed: 20049326]
31. Erol A. Visceral adipose tissue specific persistence of *Mycobacterium* tuberculosis may be reason for the metabolic syndrome. Med Hypotheses. 2008; 71:222–228. [PubMed: 18448263]
32. Pfenniger A, Chanson M, Kwak BR. Connexins in atherosclerosis. Biochim Biophys Acta. 2013; 1828:157–166. [PubMed: 22609170]
33. Warwick RA, Hanani M. The contribution of satellite glial cells to chemotherapy-induced neuropathic pain. Eur J Pain. 2013; 17:571–580. [PubMed: 23065831]
34. Shoemaker JP, Hoffman RV Jr. *Trypanosoma cruzi*: possible stimulatory factoRs) on brown adipose tissue of mice. Exp Parasitol. 1974; 35:272–274. [PubMed: 4206934]
35. Shoemaker JP, Hoffman RV Jr, Huffman DG. *Trypanosoma cruzi*: preference for brown adipose tissue in mice by the Tulahuen strain. Exp Parasitol. 1970; 27:403–407. [PubMed: 4192594]

36. Nagajyothi F, Desruisseaux MS, Machado FS, Upadhya R, Zhao D, Schwartz GJ, Teixeira MM, Albanese C, Lisanti MP, Chua SC Jr, Weiss LM, Scherer PE, Tanowitz HB. Response of adipose tissue to early infection with *Trypanosoma cruzi* (Brazil strain). J Infect Dis. 2012; 205:830–840. [PubMed: 22293433]

37. Adesse D, Garzoni LR, Huang H, Tanowitz HB, de Nazareth Meirelles M, Spray DC. *Trypanosoma cruzi* induces changes in cardiac connexin43 expression. Microbes Infect. 2008; 10:21–28. [PubMed: 18068391]

38. Brosnan CF, Scemes E, Spray DC. Cytokine regulation of gap junction connectivity - An open-and-shut case or changing partners at the nexus? Am J Pathol. 2001; 158:1565–1569. [PubMed: 11337352]

39. Duffy HS, John GR, Lee SC, Brosnan CF, Spray DC. Reciprocal regulation of the junctional proteins claudin-1 and connexin43 by interleukin-1beta in primary human fetal astrocytes. J Neurosci. 2000; 20:RC114. [PubMed: 11090614]

40. Markoullis K, Sargiannidou I, Schiza N, Hadjisavvas A, Roncaroli F, Reynolds R, Kleopa KA. Gap junction pathology in multiple sclerosis lesions and normal-appearing white matter. Acta Neuropathol. 2012; 123:873–886. [PubMed: 22484441]

41. Niger C, Howell FD, Stains JP. Interleukin-1beta increases gap junctional communication among synovial fibroblasts via the extracellular-signal-regulated kinase pathway. Biol Cell. 2010; 102:37–49. [PubMed: 19656083]

42. Cousin B, Cinti S, Morroni M, Raimbault S, Ricquier D, Penicaud L, Casteilla L. Occurrence of brown adipocytes in rat white adipose tissue: molecular and morphological characterization. J Cell Sci. 1992; 103(Pt 4):931–942. [PubMed: 1362571]

43. Lee YH, Mottillo EP, Granneman JG. Adipose tissue plasticity from WAT to BAT and in between. Biochim Biophys Acta. 2014; 1842:358–369. [PubMed: 23688783]

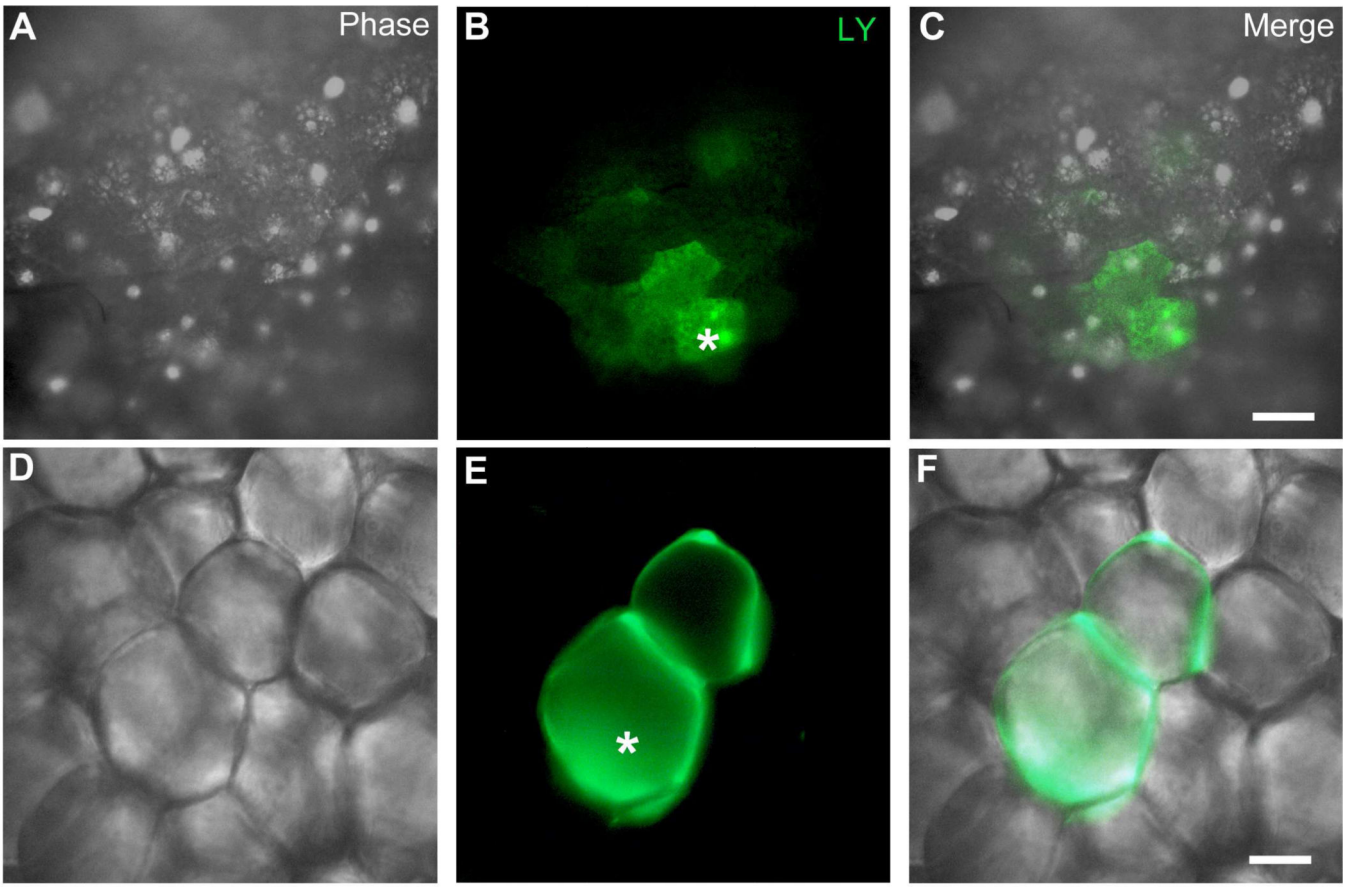

Figure 1.

Functional coupling in adipose tissue. **A–F**. Dye injection. Individual adipocytes were intracellularly injected with the fluorescent dye Lucifer yellow (LY). Asterisk indicates the injected cell. **A–C**: Brown adipose tissue (BAT) with dye coupling to neighboring cells; **D–F**: White adipose tissue (WAT) with dye spread to one neighboring cell. Scale bar = 30 μm.

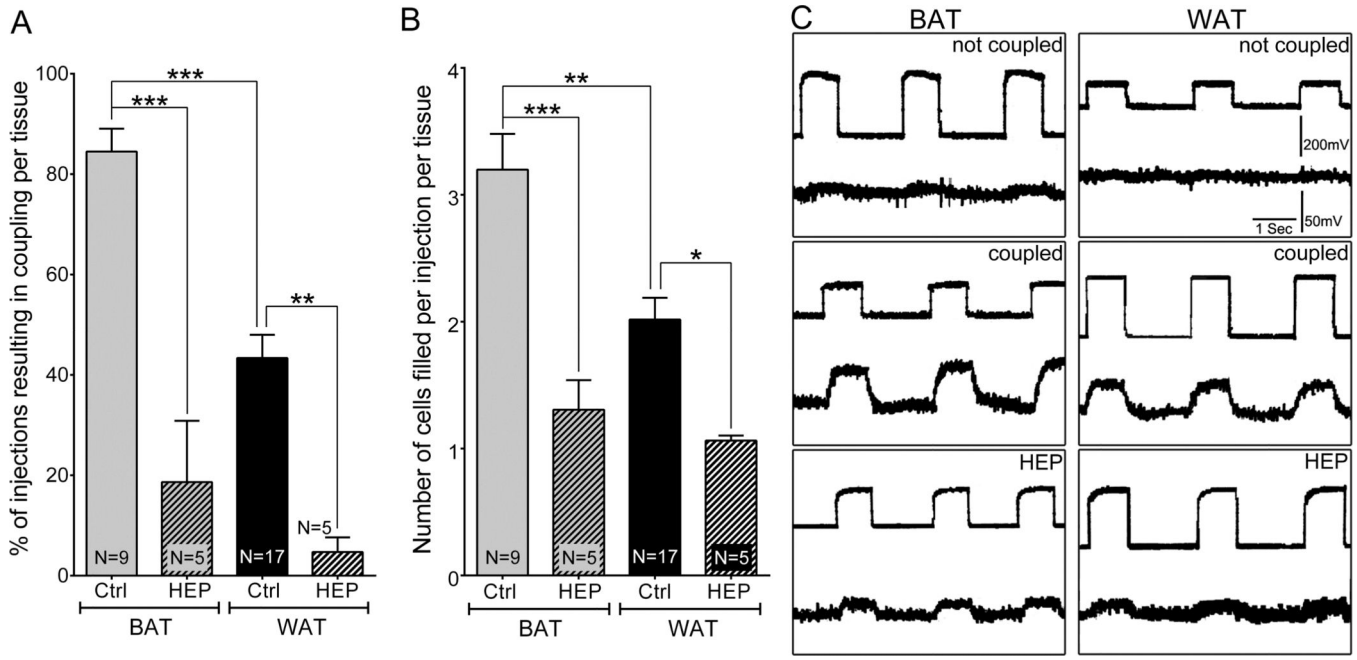

Figure 2.

Quantification of dye coupling and its blockade by the gap junction inhibitor heptanol. **A**: Graph showing the mean percentage of injections per tissue that resulted in coupling. **B**: Graph showing the mean number of cells seen in each injection per tissue sample. All data are presented as mean ± SEM, N ≥ 5. P values were obtained using one way ANOVA analysis followed by Tukey's multiple comparison test. (*P < 0.05, **P < 0.005, ***P < 0.0005, control vs. treated). **C**: Electrical coupling in brown and white adipose tissue. Current pulses were delivered into one cell and voltage deflections recorded in that cell (top) and a neighbor (bottom trace) shown by LY to be coupled to the first, injected cell. Lack of measureable current spread from electrode within the cell (upper trace) and an extracellular electrode before impalement of a second cell (not coupled), measureable spread of current when the second microelectrode was placed into a coupled cell (coupled), and significant reduction in current when tissue with the second electrode still in the same coupled cell, after the sample was incubated for 1 h with 3mM heptanol (HEP).

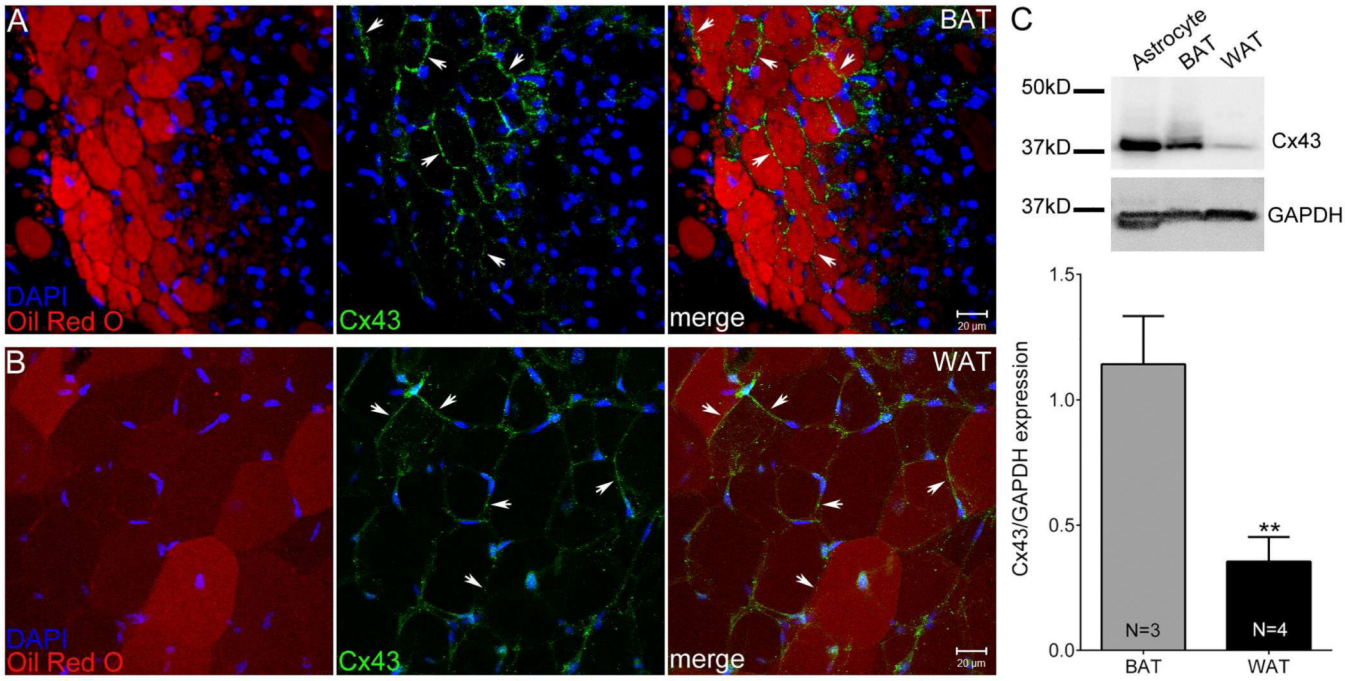

Figure 3.

Biochemical evidence for Cx43 in adipose tissue. Confocal image stacks showing Cx43 distribution (green, arrows) together with Oil-Red-O (red) and DAPI (blue) staining in (**A**) Brown adipose tissue (BAT) and (**B**) white adipose tissue (WAT). Scale bar = 20 μm. **C**. Representative Western blots of Cx43 and GAPDH in BAT and WAT and quantification of Cx43 levels normalized with respect to internal loading control GAPDH. All data are presented as mean ± SEM, (N = 3 [BAT], N = 4 [WAT]). P value was obtained using unpaired t-test. (**P < 0.005, BAT vs. WAT)

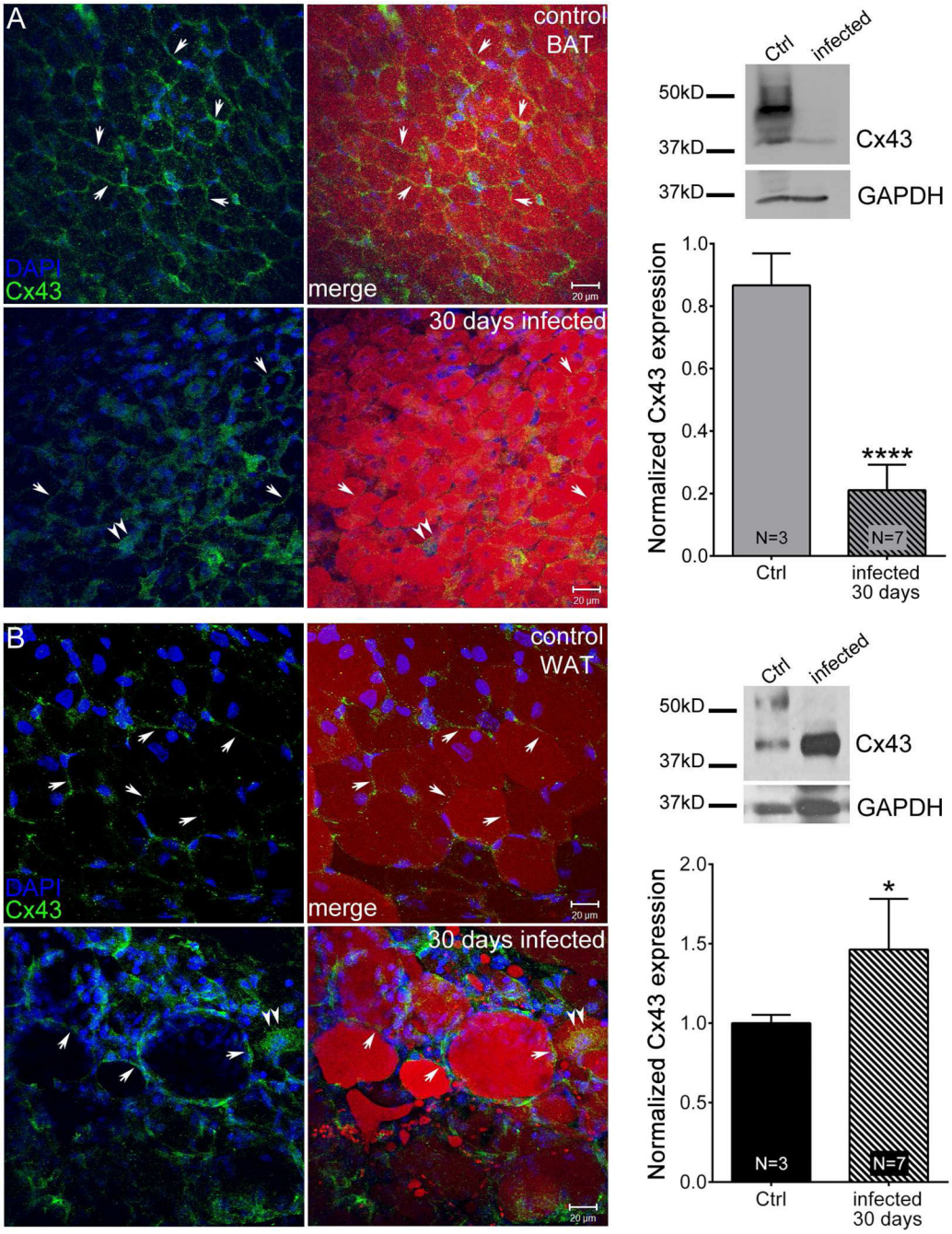

Figure 4.

Acute *T.cruzi* infection alters Cx43 distribution and expression in adipose tissue. Animals were infected with 5×10^4 Brazilian Strain *T. cruzi* for 30 days. Confocal image stacks from control brown adipose tissue (BAT) (**A,** upper panel), infected BAT (**A**, lower panel), control white adipose tissue (WAT) (**B**, upper panel) and infected WAT (**B**, lower panel) showing Cx43 distribution (green, arrows), Oil-Red-O (red) and DAPI (blue) staining. Scale bar = 20 µm. Representative Western blots and normalized expression of Cx43 from 30 day infected mice (BAT [**A**] and WAT [**B**]) compared to that of respective control. The blots

were analyzed using image J and results were normalized first to GAPDH followed by control. All data are presented as mean ± SEM. P values were obtained using unpaired t-test. (**P < 0.005, ****P < 0.00005, Control vs. infected adipose tissue)

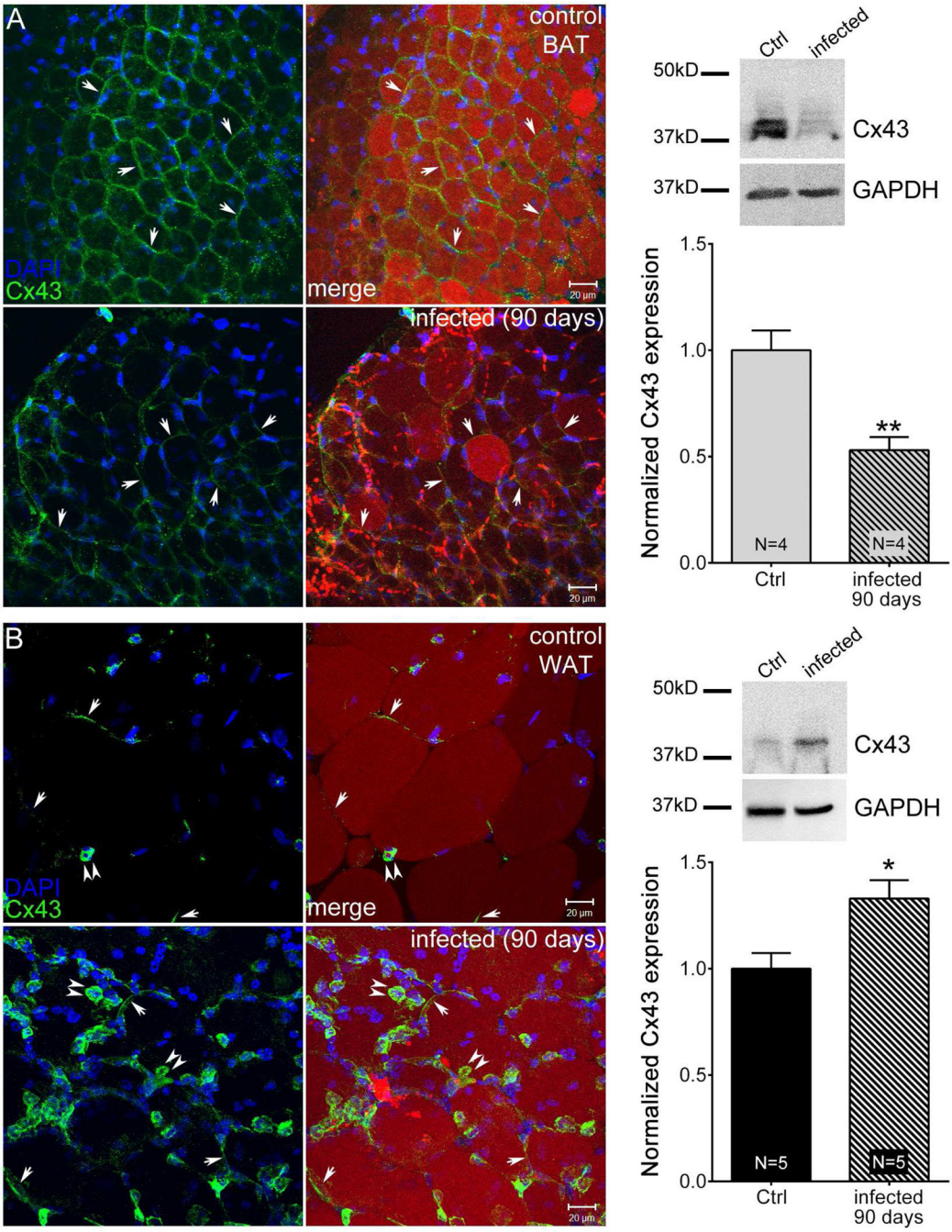

Figure 5.

Chronic *T. cruzi* infection alters Cx43 distribution and expression in adipose tissue. Animals were infected with 5×10^4 Brazilian Strain *T. cruzi* for 90 days. Stacked confocal images from control BAT (**A,** upper panel), infected BAT (**A**, lower panel), control white adipose tissue (WAT) (**B**, upper panel) and infected WAT (**B**, lower panel) showing Cx43 distribution (green, arrows), Oil-Red-O (red) and DAPI (blue) staining. Scale bar = 20 µm. Representative Western blots and normalized expression of Cx43 from 30 day infected mice (BAT [**A**] and WAT [**B**]) compared to that of respective control. The blots were analyzed

using image J and results were normalized first to GAPDH followed by control. All data are presented as mean ± SEM. P values were obtained using unpaired t-test. (*P < 0.05, **P < 0.005, Control vs. infected adipose tissue)